Available online at www.sciencedirect.com
SCIENCE DIRECT®

Journal of the European Ceramic Society 24 (2004) 2313–2318

www.elsevier.com/locate/jeurceramsoc

Effect of carbon addition on the microstructure of Si_3N_4–C_{fiber} composites using semiconductor-waste Si sludge

Byong-Taek Lee*, Dong-Hwi Jang, Taek-Soo Kim

School of Advanced Materials Engineering, Kongju National University, 182 Sinkwan-dong, Kongju City, 314-701, South Korea

Received 26 February 2003; received in revised form 10 May 2003; accepted 8 June 2003

Abstract

Si_3N_4–C_{fiber} composites using waste-Si sludge were fabricated by hot pressing at 1850 °C for 2 h with and without the addition of carbon powder. The composites were composed of small amounts of β-Si_3N_4, O′SiAlON, SiC and Y_2SiO_5 regardless of carbon powder addition. In the composite without the addition of carbon powder, most of the carbon fibers were graphitized with fine particles. Furthermore, many cavities were observed in the interior regions of C-fibers as well as at the interfaces of Si_3N_4/C_{fiber} caused by the decomposition of them. However, in the composite with 3 wt.%C powder added, the core regions of C-fibers still existed in an amorphous. The average size of a matrix grain in the composite using 3 wt.%C powder was slightly finer than that of composite fabricated without using carbon powder, which was caused by the existence of nanometer-sized SiC particles.

Keywords: Carbon; Composites; Fibres; Microstructure-final; Si_3N_4; Waste materials

1. Introduction

For the fabrication of semiconductor Si wafers, large amounts of waste-Si sludge have been generated during the cutting process of single-crystal-Si ingots. In attempts to recycle this waste-Si sludge, there have been some efforts made to produce reaction-bonded Si_3N_4 (RBSN) ceramics as well as RBSN composites.[1–3] These have some advantages, such as the low price of raw powders, the easy control of dimensions, and the low cost of production. Consequently, they have been actively developed since the removal of residual Si and pores has been made possible by post-sintering techniques such as gas-pressure-sintering (GPS).[4,5] In recent work using waste-Si powder, it was confirmed that the O′-SiAlON particles formed in the GPSed–RBSN bodies due to the high oxygen content in the raw Si powders (13.20 wt.%), which compared with that of commercial-Si powders (0.18 wt.%).[3] The formation of the O′-SiAlON phase inhibited the growth of large rod-like Si_3N_4 grains during the GPS processing, so that their mechanical properties were not improved with high values.

On the other hand, the C-fiber has been widely applied in metal matrix composites as the reinforcement because of its high mechanical properties and low cost.[6,7] Nevertheless, in the ceramic matrix composites, there were just a few reports on the fabrication and microstructure and material properties characterization of SiC or α-SiAlON systems.[8,9] The main reason is that C-fiber easily degenerated even in the inert atmosphere due to its decomposition as well as the formation of reaction compounds with the matrix phase during the high temperature processing. In general, it is considered that the decomposition of C-fiber is basically due to the reaction with oxygen that exists in the raw matrix powder. Thus, the addition of carbon powder in Si sludge powder can reduce the oxygen content due to the carbothermal reduction during the nitridation process.[10] Especially, in this case, the residual carbon powder can be changed into nano-sized SiC particles in the Si_3N_4 powder. Furthermore, from the standpoint of the improvement of wear properties[11] and the light weight of the Si_3N_4 sintered body, the realization of sound Si_3N_4–C_{fiber} composite is very attractive due to the intrinsic properties of C-fibers such as low density as

* Corresponding author. Tel.: +82-41-850-8677; fax: 82-41-858-2939.
E-mail address: lbt@kongju.ac.kr (B.-T. Lee).

0955-2219/$ - see front matter © 2003 Elsevier Ltd. All rights reserved.
doi:10.1016/S0955-2219(03)00632-0

well as the role of solid lubricant. In this paper, we report on the effect of carbon powder addition to obtain the sound Si_3N_4–3wt.%C_{fiber} composite and detailed microstructure characterization of its composite such as C-fiber, matrix and interface by TEM.

2. Experimental

The raw Si powders were obtained from the waste-Si sludge by using a vacuum filtering and sieving process.[1,3] The Si particle added 0 and 3 wt.%C carbon powders were mixed by using a ball milling process. To make the Si_3N_4 powders, the mixtures were nitrided in a flowing N_2–10%H_2 gas mixture at 1400 °C for 20 h. The synthesized Si_3N_4 powders were ground by attrition milling and then they were sieved with 100 mesh. The Si_3N_4 powder, 3 wt.% chopped-C_{fibers} (Taekwang Co., TZ-307) and sintering additives (5 wt.%Y_2O_3 and 2 wt.%Al_2O_3) were mixed in ethanol using ultrasonic power. The mixtures were dried on a hot plate while stirring and then densified by hot press at 1850 °C for 2 h under 30 MPa pressure in the Ar gas atmosphere. The XRD was used to examine the crystal phases of raw Si_3N_4 powders and Si_3N_4–3 wt.%C_{fiber} composites over a wide scale. The detailed internal microstructures and crystalline phases were examined by TEM (Jeol-2010) and electron diffraction patterns.

3. Results and discussion

Fig. 1 shows SEM images of C-fiber (a,b), waste Si (c) and RBSN powders (d) for making the Si_3N_4–3 wt.%C_{fiber} composites which were synthesized by direct nitridation using waste-Si and 3 wt.% carbon powders. The diameter and aspect ratio of chopped-C-fiber were respectively about 7 μm and 100 μm, and seen with straight and smooth surface [Fig. 1(b)]. The shape of raw Si powder, which obtained from the sieving and filtrating of waste-Si sludge, was irregular and its average size was 7 μm in diameter (c).[3] Most of the primary Si_3N_4 powders were fine, equiaxed-shape about 0.3 μm in diameter, as designated by arrowheads, although some Si_3N_4 powder was seen with aggregates of about 2–5 μm (d). The morphologies and size distribution of Si_3N_4 powder synthesized without using carbon powder were similar to those using carbon powders.

Fig. 2 shows X-ray diffraction patterns of raw C-fiber (a) and Si_3N_4 powders which were made using 0 wt.%C (b), hereafter: Si_3N_4–0C and 3 wt.%C powders (c), hereafter: Si_3N_4–3C. The profile of the C-fiber appeared with a halo pattern. Without the dependency of carbon addition, both Si_3N_4 powders were composed of multi phases (α-Si_3N_4, β-Si_3N_4 and Si_2N_2O) although the intensity of the α-Si_3N_4 peaks was remarkably stronger than that of β-Si_3N_4 peaks. The high intensity of Si_2N_2O peaks was due to the high oxygen content in

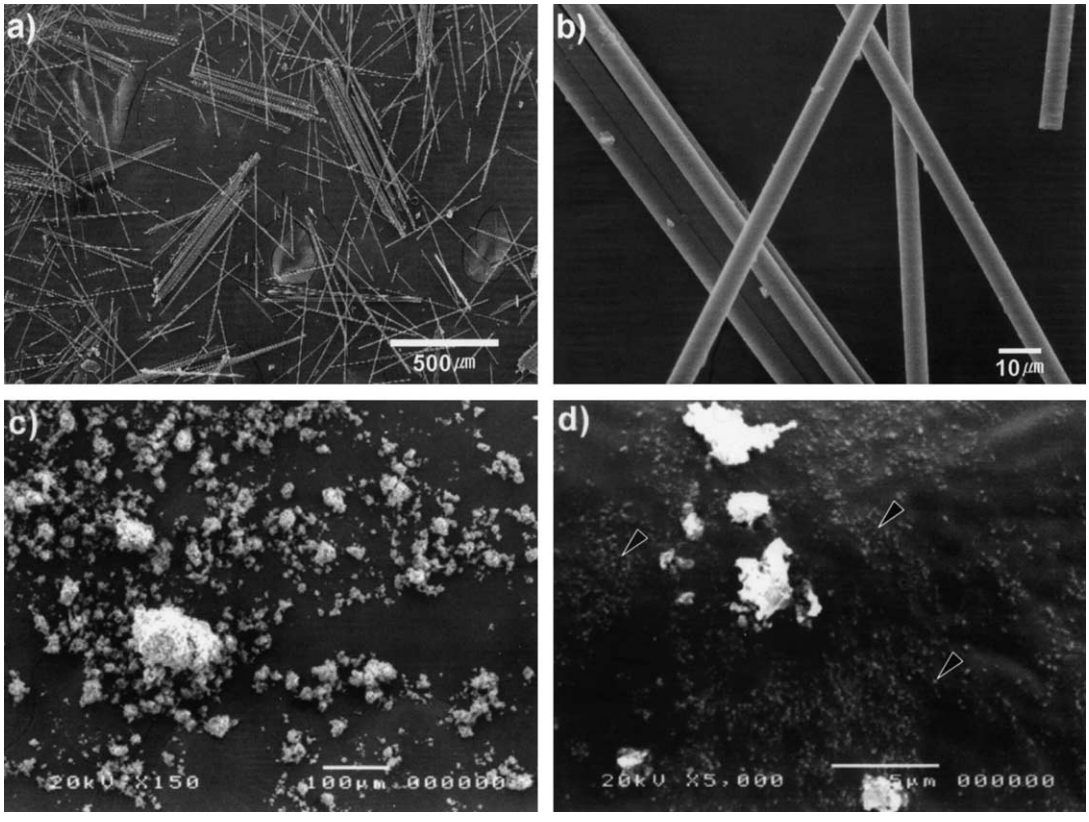

Fig. 1. SEM micrographs of C-fibers (a, b) and Si Si (c) and d) Si_3N_4 powder for making Si_3N_4–C_{fiber} composites.

semiconductor-waste-Si powders.[3] However, in the case of using commercial Si powders, the Si_2N_2O phase was not detected.[12,13] No residual Si peaks were detected in both samples without dependency of the addition of carbon powder while in Fig. 2(c), β-SiC phases were found with weak peaks causes by the addition of 3 wt.% carbon powder.

Fig. 3 is SEM images showing plasma-etched microstructures of Si_3N_4–3 wt.%C_{fiber} composites using Si_3N_4–0C (a) and Si_3N_4–3C powders (b). In the low magnified SEM observation, the C-fibers showed a homogeneous distribution. The aspect ratio of carbon fibers was remarkably decreased caused by the breaking of fibers during the mixing. In Fig. 3(a), the C-fibers seemed to receive some corrosion. Thus, some serious cavities were easily found at the interfaces between the Si_3N_4 matrix and C-fibers as indicated by arrowheads. However, in the composite using Si_3N_4–3C powder (Fig. 3(b)), the interfaces showed dense structure although a few pores were also observed at the interfaces. The average grain size of the matrix in both composites using Si_3N_4–0C and Si_3N_4–3C powders was fine with less than 2μm in diameter, which was more fine than that of GPSed-RBSN bodies using commercial Si powder.[14] Especially in the case of Si_3N_4–3C powder, the grain size was finer than that of Si_3N_4–0C powder.

Fig. 4 shows X-ray diffraction patterns of Si_3N_4–3 wt.%C_{fiber} composites using Si_3N_4–0C (a) and Si_3N_4–3C (b) powders. In both of the XRD profiles, β-Si_3N_4 and O′-SiAlON peaks were detected as the main phases while the β-SiC and Y_2SiO_5 were minor phases. The α-Si_3N_4 phase, which appeared in the raw Si_3N_4 powder, was not detected due to the α/β phase transformation during the hot pressing. From the observation of O′-SiAlON peaks instead of Si_2N_2O peaks, which were detected in the raw Si_3N_4 powders, it is thought that the Si_2N_2O phases are changed into the O′-SiAlON phase because of some dissolution of Al in the liquid phase

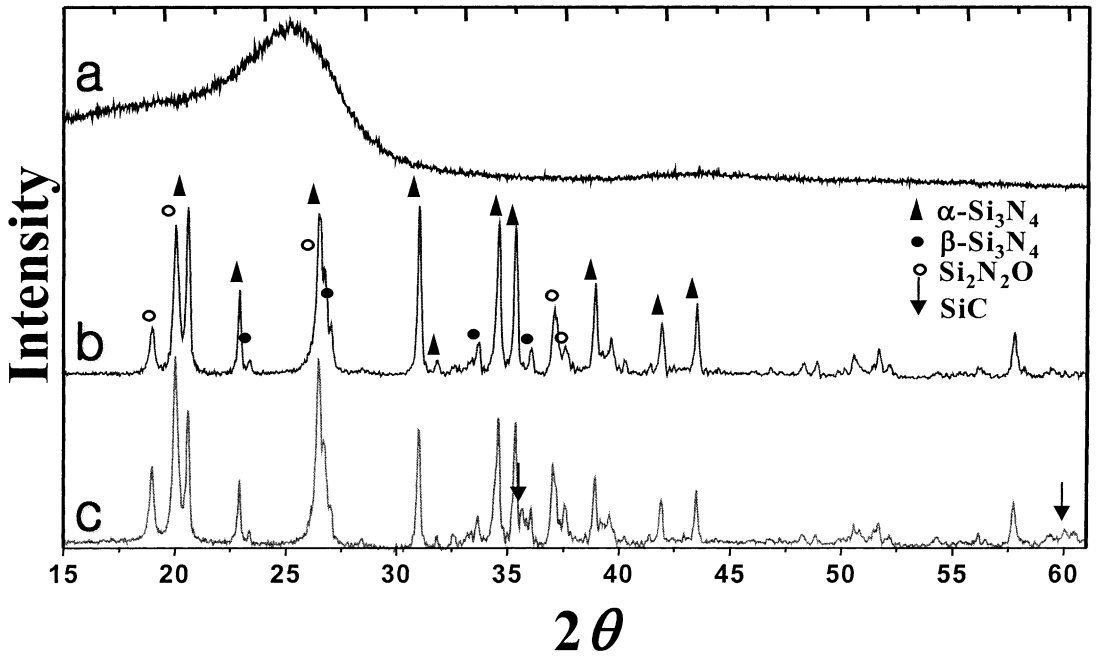

Fig. 2. XRD profiles of raw C-fiber (a) and Si_3N_4 powder synthesized without carbon (b) and with 3 wt.% carbon powders (c).

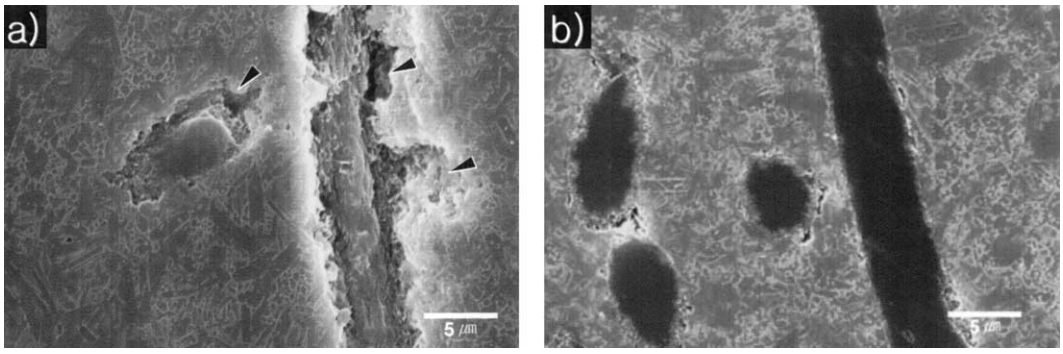

Fig. 3. SEM micrographs of Si_3N_4–3 wt.%C_{fiber} composites. (a) using Si_3N_4–0C powder, (b) using Si_3N_4–3C powder.

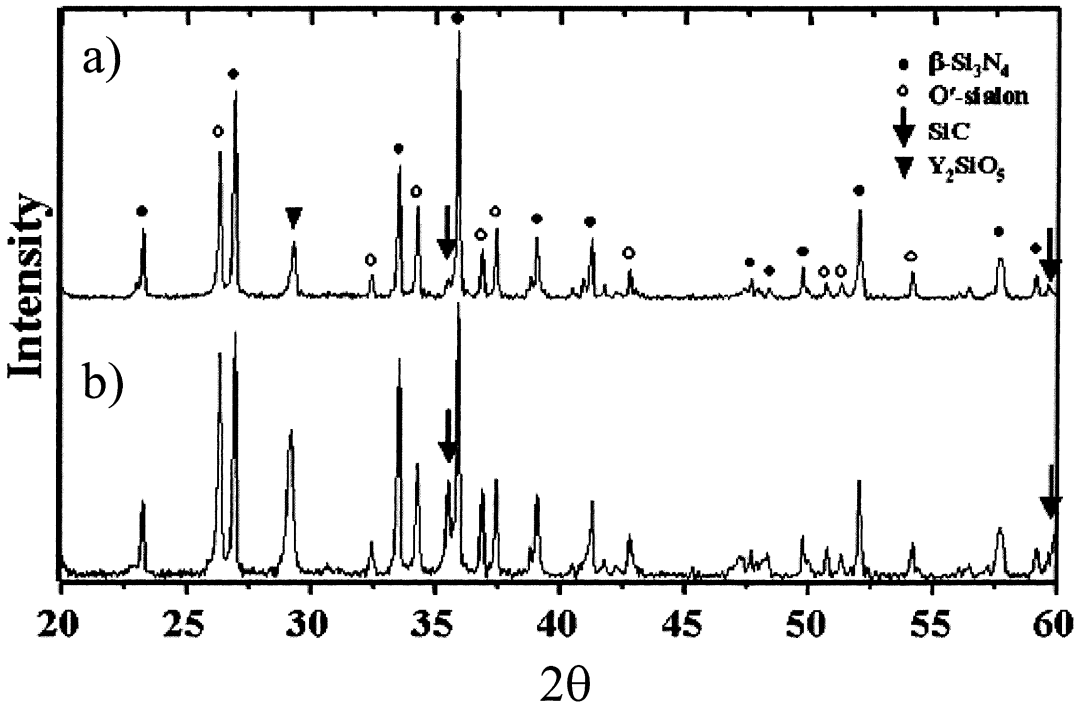

Fig. 4. XRD profiles of Si_3N_4–3 wt.%C_{fiber} composites. (a) using Si_3N_4–0C powder, (b) using Si_3N_4–3C powder.

during the hot press. An important observation is that the SiC was detected even in the composite using Si_3N_4–0C powder. In this case, the carbon source originated from the decomposition of C-fiber as shown in Fig. 3. By using Si_3N_4–3C powder, the peaks of the SiC and Y_2SiO_5 phases were stronger than those of using Si_3N_4–0C powder.

Fig. 5(a) is a TEM image showing around C-fiber in the Si_3N_4–3 wt.%C_{fiber} composite using Si_3N_4–0C powder. Most parts of C-fiber, as indicated with the dotted-line, were decomposed with graphite and SiC phase. A few fine SiC particles (50–400 nm) were observed in the interior regions of C-fibers, as marked with P. The electron diffraction pattern taken from the P region shows [110] zone axis of β-SiC. The electron diffraction pattern of Q_1 (taken from the marked Q_1 region of the interior of the C-fiber) showed a typical halo pattern that was locally observed in the interior region of the C-fiber. This result indicates that a small portion of C-fibers still existed with turbostratic structure. However, large portion of C-fibers were composed of graphite as shown in the electron diffraction pattern of Q_2. Many fine pores were also observed in the interior regions of C-fibers due to the decomposition of them, as indicated with arrowheads. A few SiC particles were also observed in the large Si_3N_4 grains located near the carbon fibers.

Fig. 6(a) is a TEM image showing the matrix. Fig. 6(b) shows a part of the C-fiber and electron diffraction patterns (c–e) which were taken from the marks c, d and e on Fig. 6(b). Many fine sized, spherical shaped SiC particles, as marked with O and P on Fig. 6(a), were homogeneously dispersed in the Si_3N_4 grains, which were located even farther from the C-fiber. This result indicated that the raw Si_3N_4–3C powder included some residual carbon even after the nitridation process, and the residual carbon led to the in-situ precipitation of nano-sized SiC particles during the hot press. The fine SiC particles also gave an effect to inhibit the grain growth of the Si_3N_4 matrix, as explained in Fig. 3. In addition, most triple regions such as marked in the Q

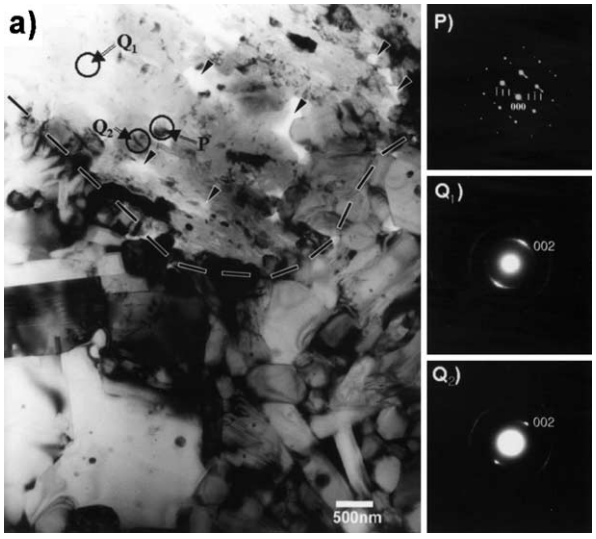

Fig. 5. TEM image (a) of Si_3N_4–3 wt.%C_{fiber} composite used Si_3N_4–0C powder. Electron diffraction patterns of (b), (c) and (d) were taken from the marked P, Q1 and Q2 regions in Fig. 5(a), respectively.

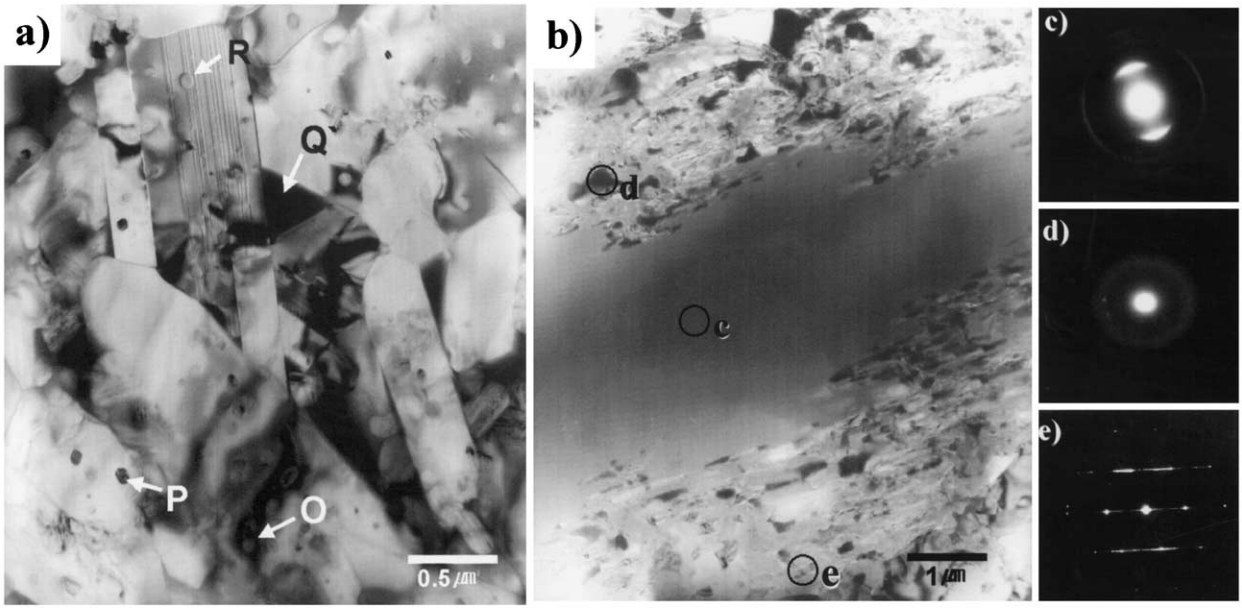

Fig. 6. (a). TEM image of matrix in the Si_3N_4–3 wt.%C_{fiber} composite using Si_3N_4–3C powder. (b) TEM image and electron diffraction patterns (c–e) of fiber regions of Si_3N_4–3 wt.%C_{fiber} composite using Si_3N_4–3C powder.

region existed with liquid phase. The marked R grain showed an O′-SiAlON phase which including many stacking faults.[15] An important observation is that the C-fiber in the central region of Fig. 6(b) still existed with turbostratic structure, as shown in the electron diffraction pattern (c). From the TEM observation, it could be understood that the addition of carbon powder caused some retardation of the decomposition of C-fibers in the Si_3N_4–3 wt.%C_{fiber} composite during the hot press. But the surface regions of the C-fiber were also decomposed with graphite and a SiC phase similar to that of Fig. 5(a). Thus, the surface regions of C-fibers revealed an open structure due to the existence of many pores and the formation of graphite and SiC particles. The electron diffraction patterns of c–e [taken from c, d and e regions of Fig. 6(b)] showed typical C-fiber, liquid phase and β-SiC, respectively. The strong streaks in the electron diffraction pattern of (e) are due to the existence of many stacking faults in the SiC particles. Small amounts of liquid phase as a sintering additive were observed locally at the surface region (d) of C-fiber due to the infiltration by the capillary effect through the many pores that were formed when the C-fiber was decomposed into SiC and graphite.

4. Conclusions

From the study on the effect of carbon addition on the microstructures of hot pressed Si_3N_4–3 wt.%C_{fiber} composites using semiconductor-waste Si sludge, the following results were obtained. The matrix in both composites using Si_3N_4–0C and Si_3N_4–3C powders comprised multiple phases including β-Si_3N_4, O′SiAlON, SiC and Y_2SiO_5 without dependency of carbon content. In the composite using Si_3N_4–0C powder, most C-fibers were decomposed with graphite and SiC; thus, many cavities were observed at the interfaces of Si_3N_4/C_{fiber} and even in their interior regions. However, in the composite using Si_3N_4–3C powder, the core regions of C-fiber still existed with amorphous phase. The average grain size of the composite using Si_3N_4-3C powder was slightly finer than that of using Si_3N_4z–0C powder (<2 μm in size), which was caused by the existence of nanometer-sized SiC particles as well as the absence of large rod-like Si_3N_4 grains.

Acknowledgements

This work was supported by the 2002NRL research program of MOST. The authors would like to acknowledge the assistance of Mr. J. H. Yoo.

References

1. Lee, B.-T., Yoo, J.-H. and Kim, H.-D., Fabrication of electroconductive Si_3N_4–TiN ceramic composites by in-situ reaction sintering. *Kor. J. Mater. Res.*, 1999, **9**, 577–582.
2. Lee, S.-Y. and Lee, B.-T., Recycling of silicon wafer cutting sludge to form silicon nitride ceramics. *Ceram. Trans.*, 1998, **93**, 51–57.
3. Lee, B.-T., Jeong, H.-G. and Hiraga, K., Microstructures and fracture characteristic of Si_3N_4–O′-SiAlON composites using waste-semiconductor Si sludge. *Mater. Trans. JIM*, 2002, **43**, 19.
4. Tiegs, N., Kiggans, J. O. and Ploetz, K. L., Application of microwave heating for fabrication of silicon nitride ceramics. *Ceram. Eng. Sci. Proc.*, 1993, **14**, 744.

5. Wang, C., Emoto, H. and Mitomo, M., Nucleation and growth of silicon oxynitride grains in a fine-grained silicon nitride matirix. *J. Am. Ceram. Soc.*, 1998, **81**, 1125–1132.
6. Vidal-Setif, M. H., Lancin, M., Marhic, C., Valle, R., Taviart, J. L., Daux, J. C. and Rabinovitch, M., On the role of brittle interfacial phases on the mechanical properties of carbon fibre reinforced Al-based matrix composites. *Mater. Sci. and Eng. A*, 1999, **272**, 321–333.
7. Korab, J., Stefanik, P., Kavecky, S., Sebo, P. and Korb, G., Thermal expansion of cross-ply and woven carbon fibre–copper matrix composites. *Compo. Part A*, 2002, **33**, 133–136.
8. Boitier, G., Vicens, J. and Chermant, J. L., Understanding the creep behavior of a 25 D C_f–SiC composite—I. Morphology and microstructure of the as-received material. *Mater. Sci. and Eng. A*, 2000, **279**, 73–80.
9. Yu, Z. B., Thompson, D. P. and Bhatti, A. R., Synergistic roles of carbon fibres and ZrO_2 particles in strengthening and toughening Li–α-sialon composites. *J. Eur. Ceram. Soc.*, 2002, **22**, 225–235.
10. Kim, H.-D., Han, B.-D., Park, D.-S., Lee, B.-T. and Becher, P. F., A novel two step sintering process to obtain a bimodal microstructure in silicon nitride. *J. Am. Ceram. Soc.*, 2002, **85**, 245–252.
11. Bianchi, V., Fournier, P., Planton, F. and Reynaud, P., Carbon fibre-reinforced(YMAS) glass–ceramic matrix composites: dry friction behaviour. *J. Eur. Ceram. Soc.*, 1999, **19**, 581–589.
12. Lee, B.-T. and Kim, H.-D., Nitridation mechanism of reacrion-bonded Si_3N_4 studied by transmission electron microscopy. *Mater. Trans. JIM*, 1996, **37**, 1547–1553.
13. Lee, B.-T., Yoo, J.-H. and Kim, H.-D., Size effect of raw Si powders on microstructures and material properties of RBSN and GPSed-RBSN bodies. *Mater. Sci. and Eng. A*, 2002, **333**, 306–313.
14. Lee, B.-T., Yoo, J. H. and Kim, H. D., Microstructural characterization of GPSed–RBSN and GPSed–Si_3N_4 ceramics. *Mater. Trans. JIM*, 2000, **41**, 312–316.
15. Ghosh, G., Vaynman, S., Fine, M. and Hsu, S., Microstructure and ambient properties of a sialon composite prepared by hot pressing and reactive sintering of Si_3N_4 coated with AI_2O_3. *J. Mater. Res.*, 1999, **14**, 881–890.